Theoretical study of the electronic spectrum of *p*-benzoquinone

Rosendo Pou-Amérigo, Manuela Merchán, and Enrique Ortí
Departament de Química Física, Universitat de València, Doctor Moliner, 50, E-46100 Burjassot (València), Spain

(Received 11 December 1998; accepted 19 February 1999)

The electronic excited states of *p*-benzoquinone have been studied using multiconfigurational second-order perturbation theory (CASPT2) and extended atomic natural orbital (ANO) basis sets. The calculation of the singlet–singlet and singlet–triplet transition energies comprises 19 valence singlet excited states, 4 valence triplet states, and the singlet $3s$,$3p$, and $3d$ members of the Rydberg series converging to the first four ionization limits. The computed vertical excitation energies are found to be in agreement with the available experimental data. Conclusive assignments to both valence and Rydberg states have been performed. The main features of the electronic spectrum correspond to the $\pi\pi^*$ $1\,^1A_g \rightarrow 1\,^1B_{1u}$ and $\pi\pi^*$ $1\,^1A_g \rightarrow 3\,^1B_{1u}$ transitions, computed to be at 5.15 and 7.08 eV, respectively. Assignments of the observed low-energy Rydberg bands have been proposed: An $n \rightarrow 3p$ transition for the sharp absorption located at ca. 7.4 eV and two $n \rightarrow 3d$ and $\pi \rightarrow 3s$ transitions for the broad band observed at ca. 7.8 eV. The lowest triplet state is computed to be an $n\pi^*$ $^3B_{1g}$ state, in agreement with the experimental evidence. © *1999 American Institute of Physics.* [S0021-9606(99)30419-0]

I. INTRODUCTION

p-Benzoquinone is the parent molecule of a class of compounds which play a relevant role in biological systems and in the formation of charge-transfer salts. Derivatives of this molecule have been recognized as important electron-transfer agents in biology. Plastoquinones and ubiquinones, for instance, function as electron acceptors in the photosynthetic reaction center and in the process of oxidative phosphorylation.[1] Other derivatives, such as topa-quinone, are involved as redox cofactors in the so-called quinoenzymes.[2] *p*-Quinones are also present in biochemically active sites of anthracyclines, a family of compounds of great biomedical importance due to their antitumor activity.[3] On the other hand, most of the organic conductors based on charge-transfer complexes contain a *p*-benzoquinone derivative as the acceptor component.[4]

As a consequence of the attention that *p*-benzoquinone derivatives have attracted in so many different fields, the electronic structure of *p*-benzoquinone, the simplest *para*-quinone, has been extensively studied. It represents a simple model which may provide insight into the important role that this class of compounds plays in chemistry and biochemistry. Its electronic spectrum has been the subject of numerous investigations since the 1920's, when the first quantitative study in the vapor phase and in several liquid solutions was carried out.[5] A detailed knowledge of the nature and ordering of its excited states is required for the understanding of its photophysics[6] and photochemistry.[7] Analyses of the absorption and emission spectra in a large variety of environments (in the vapor phase, in pure and mixed crystals, in solid rare gas hosts, in rigid glasses, etc.), as well as excitation spectra in a supersonic jet, are now available. (For a recent review of the experimental and theoretical studies on the excited electronic states of this molecule, see Ref. 6. Reviews of the experimental work can be also found, for instance, in Refs. 8 and 9.)

From a theoretical point of view, the nature and location of the excited states have been mostly analyzed by employing semiempirical methods.[6] These studies have been useful for the assignment of important bands of the spectrum.[8,9] However, only a few studies have dealt with these problems by using *ab initio* procedures. Wood[10] reported self-consistent field (SCF) and singly excited configuration interaction (SCI) results employing minimal basis sets of Slater type orbitals (STO-4G) for five singlet and eight triplet excited states of *p*-benzoquinone. CI calculations were also carried out by Ha,[11] using a double-zeta (DZ) basis set. All singly and doubly excited configurations considering the valence-shell electrons, based on both one-reference configuration (SDCI) and multireference wave functions (MRSDCI), were included. His analysis comprised eight singlet and six triplet excited states. The remaining *ab initio* studies were limited only to a few excited states. Martin and Wadt[12,13] examined the two lowest-lying singlet and triplet excited states ($^1B_{1g}$, ^1A_u, $^3B_{1g}$, and ^3A_u) by employing an alternative approach for the computation of excitation energies, i.e., a valence-bond model based on a nonorthogonal two-configuration wave function involving broken-symmetry SCF solutions, using minimal and DZ basis sets. Ball and Thomson[14] studied two triplet excited states ($^3B_{1g}$ and $^3B_{1u}$). They carried out geometry optimizations for the excited states at different Hartree–Fock levels, employing STO-3G and 3-21G basis sets. Optimized geometries of the molecule in the $^3B_{1g}$ state and vibrational analyses were also recently reported by Mohandas and Umapathy,[15] who employed the unrestricted Hartree–Fock method as well as several density-functional procedures and a 6-31G*(d,p)* basis set. Optimization of the molecular geometry of *p*-benzoquinone in the lowest triplet state was also per-

formed by Eriksson *et al.*[16] at the B3LYP/6-311G*(d,p)* level.

Despite the useful information these calculations yield, they do not provide a full interpretation of the electronic spectrum of *p*-benzoquinone. Computed excitation energies exhibit significant deviations from the experimental data in certain cases, even when computationally demanding procedures, like MRSDCI, are used.[11] Surprisingly, the important valence transition responsible for the prominent peak detected at 7.1 eV has not been yet studied with *ab initio* methods. No theoretical information about Rydberg states is available. In addition, a controversial issue concerns the nature of the lowest triplet state, which has been proven to be of $n\rightarrow\pi^*$ type.[9] SCF as well as SCI calculations predicted, however, a lowest triplet state with $\pi\rightarrow\pi^*$ character.[10] Inclusion of additional correlation effects through the MRSDCI procedure did not change the conclusion.[11]

In this paper, we present an extensive *ab initio* study of the electronic transitions of *p*-benzoquinone in order to answer the unresolved questions and to give quantitatively reliable vertical excitation energies for the main valence and Rydberg states. The multiconfigurational second-order perturbation (CASPT2) method[17–19] has been used for the calculation of the electronic states. This method has been demonstrated to be a valuable tool for the computation of differential correlation effects on excitation energies. Its ability to provide accurate predictions and reliable interpretations of the electronic spectra of organic molecules has also been shown in numerous applications.[20–22]

II. METHODS AND COMPUTATIONAL DETAILS

As a first step, the ground state geometry of *p*-benzoquinone was optimized by employing the complete active space (CAS)SCF approximation.[23] The active space comprised the π and π^* valence molecular orbitals (8 MOs and 8 electrons). Calculations were carried out within D_{2h} symmetry, according to the experimental data.[24] The molecule was placed in the yz plane, with the two oxygen atoms along the z axis. Generally contracted basis sets of atomic natural orbital (ANO) type were used. They were obtained from C,O$(14s9p4d)$/H$(8s4p)$ primitive sets by employing the contraction scheme C,O$[4s3p1d]$/H$[2s1p]$.[25] This basis set has been shown in previous studies to be flexible enough for a proper description of ground and valence excited states.[26,27]

As a second step, the vertical excitation energies of *p*-benzoquinone were computed. The molecule shows an electronic structure with the four highest occupied MOs (two π and two n orbitals) close in energy. This gives rise to Rydberg series converging to four ionization limits. The balanced representation of the Rydberg excited states requires an enlargement of the basis set. According to the procedure explained elsewhere,[20] the basis set was supplemented with a set of specifically designed $1s1p1d$ Rydberg-type functions contracted from a set of $8s8p8d$ primitives, placed at the center of the molecule. Four states of the *p*-benzoquinone cation were included in the average procedure to build the Rydberg functions.[20] They correspond to the states which are mainly described with an even electron located on a π orbital ($^2B_{1g}$, $^2B_{3u}$) and on an n-type orbital ($^2B_{3g}$, $^2B_{2u}$). Therefore, unless otherwise stated, a total number of 173 basis functions were used in the calculation of the electronic states.

The vertical excitation energies have been computed by means of the CASPT2 approach.[17–19] In this method, the first-order wave function and the second-order energy in full CI space are calculated using the CASSCF wave function as reference. This reference includes all strongly interacting configurations and the remaining (dynamic) correlation effects are taken into account in the second-order perturbation treatment. Numerous previous studies have shown that this procedure yields accurate excitation energies.[20–22] Based on the experience gained for systems with the molecular size equivalent to that of *p*-benzoquinone, deviations less than ± 0.2 eV with respect to experimental data can be expected for correctly correlated transitions. In the CASSCF calculation, the carbon and oxygen $1s$ electrons were kept frozen in the form determined by the ground state SCF wave function. They were not correlated at the second-order level.

Transitions of $\pi\rightarrow\pi^*$ character are expected to be related to the most intense features of the singlet–singlet spectrum. The π valence active space, which comprises eight active electrons and eight active orbitals (four π and four π^* functions), is the natural choice to perform the calculations. The π valence active space will be denoted by (8/03010301), where the first label gives the number of active electrons and the following labels indicate the number of active orbitals in each of the eight irreducible representations (a_g, b_{3u}, b_{2u}, b_{1g}, b_{1u}, b_{2g}, b_{3g}, and a_u) of the D_{2h} symmetry point group. Nevertheless, additional valence transitions are also important for the interpretation of the spectrum, such as the $n\rightarrow\pi^*$ transitions, which are responsible for the absorptions in the visible region. To compute this type of excitations, the n orbitals were added to the active space. According to the labeling explained above, it will be denoted by (12/03110311).

In order to compute Rydberg states, the active space was extended to include the $3s$,$3p$, and $3d$ orbitals. Inclusion of nine orbitals would yield an excessively large active space. However, the high symmetry of the molecule makes it possible to design partitions of this set of orbitals. As mentioned above, four series of Rydberg states are considered: Two of them resulting from excitation from the two highest occupied π orbitals and the other two from excitations from the two n orbitals. The active space employed for the first two series was constructed by adding selected sets of Rydberg orbitals to the (8/03010301) π-valence space. For the other two series, the appropriate Rydberg orbitals were added to the (12/03110311) set. Each series was treated independently. Only the required Rydberg orbitals, according to the symmetry of a given state, were included. The active spaces employed for the computation of the excited singlet states of *p*-benzoquinone, the number of configuration state functions (CSFs), and the number of state-averaged CASSCF roots are shown in Table I. The calculation of the valence singlet states was carried out simultaneously with the Rydberg states. In a few cases, extra orbitals had to be included in the active space to minimize the effect of intruder states in the CASPT2 calculations. All excitation energies were obtained

TABLE I. CASSCF wave functions employed to compute the valence and Rydberg singlet excited states of *p*-benzoquinone.

Active space[a]	States	Config.[b]	N_{states}[c]
8/03020301	$^1A_g(V_{11}, V_{18}, H\rightarrow 3d_{xy})$	1374	4
8/04010301	$^1A_g(H\text{-}1\rightarrow 3p_x)$	1402	5
12/03110321	$^1A_g(V_4, V_{19}, n_-\rightarrow 3d_{yz})$	8000	6
12/03210311	$^1A_g(n_+\rightarrow 3p_y)$	8000	6
8/33010301	$^1B_{3u}(H\text{-}1\rightarrow 3s, 3d_{x^2-y^2}, 3d_{z^2})$	4128	3
12/03120312	$^1B_{3u}(V_7, n_+\rightarrow 3d_{xy})$	27 680	2
12/23110301	$^1B_{3u}(H\rightarrow 3p_y)$	4060	2
8/04010301	$^1B_{2u}(V_{13}, H\rightarrow 3p_x)$	1274	3
8/03020301	$^1B_{2u}(H\text{-}1\rightarrow 3d_{xy})$	1302	2
12/03111311	$^1B_{2u}(n_-\rightarrow 3p_z)$	7588	1
12/33110311	$^1B_{2u}(n_+\rightarrow 3s, 3d_{x^2-y^2}, 3d_{z^2})$	91 818	4
8/33210301	$^1B_{1g}(H\rightarrow 3s, 3d_{x^2-y^2}, 3d_{z^2})$	17 799	4
8/23110301	$^1B_{1g}(H\text{-}1\rightarrow 3p_y)$	4004	2
12/03110411	$^1B_{1g}(V_1, V_9, V_{16}, n_-\rightarrow 3d_{xz})$	7588	6
12/04110311	$^1B_{1g}(n_+\rightarrow 3p_x)$	7588	3
8/03010501	$^1B_{1u}(V_6, V_{14}, V_{15}, H\text{-}1\rightarrow 3d_{xz})$	3520	4
12/03210311	$^1B_{1u}(n_-\rightarrow 3p_y)$	7800	4
12/03110321	$^1B_{1u}(n_+\rightarrow 3d_{yz})$	7800	4
8/03011311	$^1B_{2g}(H\text{-}1\rightarrow 3p_z)$	1680	1
8/03012311	$^1B_{2g}(H\rightarrow 3d_{yz})$	4060	2
12/03120311	$^1B_{2g}(V_5, V_8, n_-\rightarrow 3d_{xy})$	7396	4
8/03010501	$^1B_{3g}(V_3, V_{12}, H\rightarrow 3d_{xz})$	3360	4
12/03111311	$^1B_{3g}(n_+\rightarrow 3p_z)$	7588	3
12/33111311	$^1B_{3g}(n_-\rightarrow 3s, 3d_{x^2-y^2}, 3d_{z^2})$	267 960	5
8/03011301	$^1A_u(H\rightarrow 3p_z)$	574	1
8/03010311	$^1A_u(H\text{-}1\rightarrow 3d_{yz})$	602	1
12/03110412	$^1A_u(V_2, V_{10}, V_{17}, n_+\rightarrow 3d_{xz})$	27 832	4
12/04110311	$^1A_u(n_-\rightarrow 3p_x)$	7588	4

[a]Number of active electrons/number of active orbitals of symmetry a_g, b_{3u}, b_{2u}, b_{1g}, b_{1u}, b_{2g}, b_{3g}, and a_u, respectively.
[b]Number of CSFs.
[c]Number of state-averaged CASSCF roots.

using the ground state energy computed with the same active space as was used in the calculation of the corresponding excited states.

The transition dipole moments were computed by using the CASSCF state interaction (CASSI) method, which enables an efficient calculation of the transition properties for nonorthogonal state functions.[28,29] Energy differences corrected by CASPT2 correlation energies were used in the oscillator strength formula. All calculations have been performed with the MOLCAS-4 program package.[30]

III. RESULTS AND DISCUSSION

A. Geometry optimization

The equilibrium geometrical parameters computed at the π-CASSCF level for the ground state of *p*-benzoquinone are listed in Table II. For the sake of comparison, available experimental data derived from electron diffraction measurements[24] are also included. The bond-length alternancy found for the carbon–carbon bonds clearly reveals the quinoidal character of this molecule. Experimentally, two of them have bond distances of a typical value for a C=C double bond (1.34 Å), whereas the four remaining bonds exhibit longer distances (1.48 Å), which lie within the range expected for a C–C single bond. These bond lengths are different from those observed for benzene (1.395 Å),[31] but

TABLE II. Geometrical parameters for the ground state of *p*-benzoquinone optimized at the π–CASSCF level.

Parameter[a]	CASSCF	Exp.[b]
r(C=O)	1.210	1.225±0.002
r(C=C)	1.343	1.344±0.003
r(C—C)	1.479	1.481±0.002
r(C—H)	1.074	1.089±0.011
∠(C—C—C)	117.4	118.1±0.3
∠(C=C—H)	122.2	(121.4)[c]

[a]Bond distances in Å and angles in degrees.
[b]Gas-phase electron diffraction data (Ref. 24).
[c]Assumed value.

are close to the data determined for 1,4-cyclohexadiene (1.33–1.35 Å for double bonds and 1.49–1.52 Å for single bonds).[32,33] For *p*-benzoquinone, the C=O bond length (1.225 Å) is similar to that obtained for other ketones such as acetone (1.222 Å).[34]

The computed parameters shown in Table II are in agreement with the available experimental data. As expected, the theoretical parameters support the gas-phase electron diffraction data.[24] Nevertheless, as can be noted in Table II, the carbon–oxygen bond is 0.015 Å shorter than the derived experimental value. Two possible sources can be invoked to explain such a discrepancy. One is that the C=O bond distance is particularly sensitive to electron correlation effects, and the other is that the data derived from electron diffraction are not free from the assumptions and limitations used.[35,36] The previously available SCF calculations, employing large basis sets, predict a bond length of 1.194–1.196 Å,[15,37–40] which is about 0.03 Å shorter than the experimental value. Inclusion of electron correlation effects by means of the MP2 approach results in an overestimation of the C=O bond length by 0.012–0.016 Å.[38–43] The CASSCF method leads, however, to a somewhat shorter C=O bond distance compared to the experimental data.

B. Qualitative analysis

In order to achieve an understanding of the most important features of the electronic spectrum of *p*-benzoquinone presented later, an analysis of the molecular orbitals (MOs) distribution can be helpful. The orbital energy levels close to the highest occupied MO (HOMO) and lowest unoccupied MO (LUMO) calculated at the SCF level are depicted in Fig. 1. The six highest occupied molecular orbitals correspond to four π orbitals and two *n* orbitals. The *n* orbitals are described essentially by either the symmetric (n_+) or antisymmetric combination (n_-) of the $2p_y$ atomic orbitals on the oxygen atoms. The electronic spectrum of *p*-benzoquinone is determined to a large extent by the four highest occupied orbitals, which are separated by more than 2.5 eV from the remaining. At this level of calculation, the HOMO and HOMO-1 are computed to be of π nature. Next, in decreasing ordering of orbital energies the lone-pairs of the oxygens, n_- (HOMO-2) and n_+ (HOMO-3), are located. The calculation places the four orbitals within a narrow energy range, with small splittings between the two *n* levels and between the two π one-electron functions. Due to this unique struc-

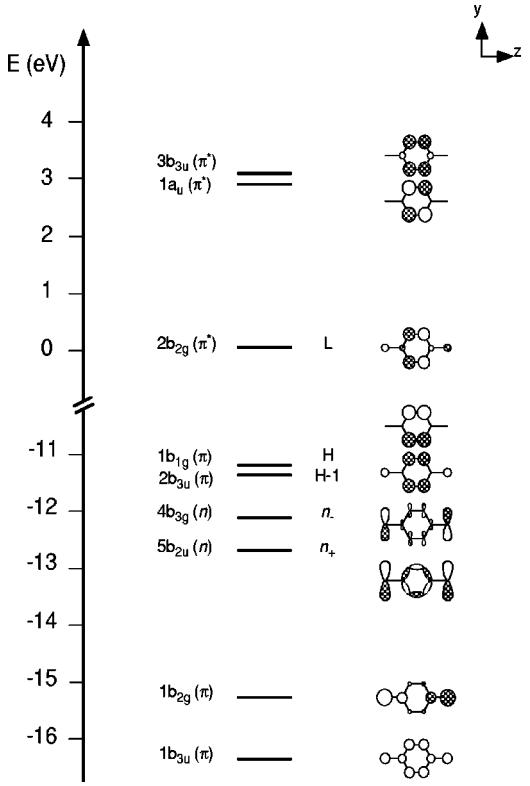

FIG. 1. Schematic diagram showing the π and n molecular orbitals distribution near the HOMO-LUMO gap of *p*-benzoquinone. The atomic orbital composition of the MOs is displayed on the right.

ture, a number of electronic transition energies and ionization potentials are expected to be found also in a narrow region. In this sense, it is worth mentioning the difficulties found in the assignment of certain bands of the electronic spectrum.[6] Likewise, the interpretation of the photoelectron spectrum of *p*-benzoquinone has given rise to an important controversy.[44] Several assignments have been proposed for the first bands, since four ionization energies have been found in a small energy range, 10–11 eV.[45]

As shown in Fig. 1, the LUMO corresponds to an antibonding π^* orbital ($2b_{2g}$). The remaining valence antibonding π^* orbitals ($1a_u$, $3b_{3u}$, and $3b_{2g}$) have a pronounced spacing with respect to the LUMO. In spite of its qualitative character, the MOs distribution obtained at the SCF level represents a useful tool for the interpretation of the findings obtained by using more advanced (and complex) wave functions.

C. Vertical excited states

The results obtained by means of the CASSCF/CASPT2 procedure are collected in Table III. The first column identifies the different excited states of *p*-benzoquinone. The character of the state is shortly described within parentheses. The singlet and triplet valence states have been labeled as *V* and *T*, respectively. The description of the valence states is supplemented by indicating the $\pi\pi^*$ or $n\pi^*$ character of the CASSCF wave function. In the case of Rydberg states, the two orbitals involved in the corresponding one-electron promotion are given. The second and third columns report the vertical excitation energies computed at CASSCF and CASPT2 levels, respectively. The difference between the two energies is a measure of the contribution of the dynamic correlation to the energy of a state. The available experimental data are listed in column 4. Column 5 collects the calculated oscillator strengths, together with the available experimental values.[46]

The CASSCF wave functions calculated for the valence singlet states of *p*-benzoquinone are summarized in Table IV. The configurations with coefficients larger than 0.05 have been classified into four groups, according to the number of excitations with respect to the main configuration of the ground state. The number of configurations and the weights for each group are reported on the left-hand side of the table. The principal configurations are listed, together with their weights, on the right part. In order to simplify the notation, they are described as electronic excitations from the principal configuration of the ground state.

1. Valence excited singlet states

a. The $1\,^1B_{1g}$ *and* $1\,^1A_u$ *states.* The two lowest-lying singlet excited states (V_1 and V_2) are of B_{1g} and A_u symmetry. The states are predicted to be degenerate at the CASPT2 level. The CASSCF wave functions are dominated by $n\rightarrow\pi^*$ one-electron excitations, $4b_{3g}\rightarrow 2b_{2g}$ ($1\,^1B_{1g}$) and $5b_{2u}\rightarrow 2b_{2g}$ ($1\,^1A_u$) (cf. Table IV). In terms of the one-electron levels (see Fig. 1), they correspond to the promotions $n_-\rightarrow L$ and $n_+\rightarrow L$, respectively. The computed vertical excitation energy, 2.50 eV, is in agreement with the available experimental data, 2.48–2.49 eV.[8,47] The two transitions, $1\,^1A_g\rightarrow 1\,^1B_{1g}$ and $1\,^1A_g\rightarrow 1\,^1A_u$, are electric-dipole forbidden. They derive most of the intensity by vibronic interaction with the higher-energy allowed $\pi\pi^*$ states through the activity of out-of-plane vibrations.[9]

The assignment of the absorption bands in the lowest-energy region of the spectrum to the $n_\pm\rightarrow L$ transitions was already proposed in the 1950's on the basis of simple molecular orbital analysis[48] and semiempirical calculations.[49] This fact did not avoid the controversy concerning the interpretation of the vibronic bands detected in the vapor phase absorption spectrum and the exact position of the corresponding origins for the two transitions.[8,50,51] With the help of the absorption spectra of the single crystal[9,52–55] and in Ne host[56] at low-temperature, this problem was partially overcome. The reduction of the symmetry induced by the crystal field allowed detection of new bands. A subsequent study of the singlet $n\pi^*$ excitation spectra in a supersonic jet[47] afforded accurate determinations of the origins of both transitions. They were found to be quasidegenerate, with the ^1A_u state below the $^1B_{1g}$ state and a splitting of 54 cm^{-1}.

Previous *ab initio* calculations predicted the $1\,^1B_{1g}$ and $1\,^1A_u$ states as the lowest singlet excited states of *p*-benzoquinone,[10,11] with the exception of SCF/DZ calculations, which placed a $\pi\pi^*$ singlet excited state of B_{3g} symmetry between the two $n\pi^*$ states.[11] At the SCF level, the computed excitation energies were found to be too high, by more than 2 eV, with a large $^1B_{1g}-{}^1A_u$ splitting.[10–13] Inclusion of correlation by means of CI procedures considerably reduced the transition energies and the splitting.[10,11,13] For

TABLE III. Computed vertical excitation energies and oscillator strengths for the electronic states of *p*-benzoquinone. Experimental data are also included.

State	Excitation energies (eV)			Osc. Str.[a]
	CASSCF	CASPT2	Exp.	
Singlet states				
$1\,^1A_g$				
$1\,^1B_{1g}$ $(V_1, n\pi^*)$	3.88	2.50	2.48,[b] 2.49[c]	⋯
$1\,^1A_u$ $(V_2, n\pi^*)$	3.84	2.50	2.48[c]	⋯
$1\,^1B_{3g}$ $(V_3, \pi\pi^*)$	6.11	4.19	4.07[d]	⋯(0.005±0.001)[e]
$2\,^1A_g$ $(V_4, n\pi^*)$	6.17	4.41		⋯
$1\,^1B_{2g}$ $(V_5, n\pi^*)$	6.87	4.80		⋯
$1\,^1B_{1u}$ $(V_6, \pi\pi^*)$	7.81	5.15	5.12[d]	0.6160 (0.44±0.05)[e]
$1\,^1B_{3u}$ $(V_7, n\pi^*)$	6.92	5.15		0.0002
$2\,^1B_{2g}$ $(V_8, n\pi^*)$	9.37	5.49		⋯
$2\,^1B_{1g}$ $(V_9, n\pi^*)$	7.22	5.76		⋯
$2\,^1A_u$ $(V_{10}, n\pi^*)$	7.22	5.79		⋯
$3\,^1A_g$ $(V_{11}, \pi\pi^*)$	7.04	5.90		⋯
$2\,^1B_{3g}$ $(V_{12}, \pi\pi^*)$	8.84	6.34		⋯
$3\,^1B_{3g}$ $(n_- \rightarrow 3s)$	8.32	6.53		⋯
$2\,^1B_{1u}$ $(n_- \rightarrow 3p_y)$	9.11	6.86		0.0127
$1\,^1B_{2u}$ $(V_{13}, \pi\pi^*)$	8.30	6.89		0.0219
$3\,^1B_{1u}$ $(V_{14}, \pi\pi^*)$	10.45	7.08	7.1[e]	0.6243 (0.81±0.10)[e]
$4\,^1A_g$ $(n_+ \rightarrow 3p_y)$	9.12	7.08		⋯
$2\,^1B_{2u}$ $(n_+ \rightarrow 3s)$	7.91	7.10		0.0038
$4\,^1B_{1u}$ $(V_{15}, \pi\pi^*)$	8.72	7.24		0.0297
$4\,^1B_{3g}$ $(n_+ \rightarrow 3p_z)$	8.87	7.27		⋯
$3\,^1B_{1g}$ $(n_+ \rightarrow 3p_x)$	8.44	7.33		⋯
$4\,^1B_{1g}$ $(V_{16}, n\pi^*)$	8.98	7.36		⋯
$3\,^1A_u$ $(n_- \rightarrow 3p_x)$	8.50	7.36		⋯
$4\,^1A_u$ $(V_{17}, n\pi^*)$	8.97	7.39		⋯
$3\,^1B_{2u}$ $(n_- \rightarrow 3p_z)$	8.25	7.44	7.4[e]	0.0171 (0.03)[f]
$5\,^1A_g$ $(V_{18}, \pi\pi^*)$	8.77	7.46		⋯
$5\,^1B_{3g}$ $(n_- \rightarrow 3d_{x^2-y^2})$	9.25	7.62		⋯
$5\,^1B_{1g}$ $(H \rightarrow 3s)$	8.01	7.70		⋯
$5\,^1B_{1u}$ $(n_+ \rightarrow 3d_{yz})$	9.86	7.79	7.8[e]	0.0290 (0.03)[f]
$5\,^1A_u$ $(n_+ \rightarrow 3d_{xz})$	9.18	7.82		⋯
$6\,^1A_g$ $(V_{19}, n\pi^*)$	9.63	7.85		⋯
$4\,^1B_{2u}$ $(n_+ \rightarrow 3d_{x^2-y^2})$	8.81	7.87		0.0002
$7\,^1A_g$ $(n_- \rightarrow 3d_{yz})$	9.74	7.91		⋯
$6\,^1B_{3g}$ $(n_- \rightarrow 3d_{z^2})$	9.51	7.94		⋯
$2\,^1B_{3u}$ $(H\text{-}1 \rightarrow 3s)$	8.11	8.01		0.0246
$6\,^1B_{1g}$ $(n_- \rightarrow 3d_{xz})$	9.30	8.02		⋯
$3\,^1B_{2g}$ $(n_- \rightarrow 3d_{xy})$	9.12	8.12		⋯
$3\,^1B_{3u}$ $(n_+ \rightarrow 3d_{xy})$	8.84	8.17		0.0004
$8\,^1A_g$ $(H\text{-}1 \rightarrow 3p_x)$	8.92	8.18		⋯
$5\,^1B_{2u}$ $(n_+ \rightarrow 3d_{z^2})$	9.07	8.20		0.0039
$4\,^1B_{3u}$ $(H \rightarrow 3p_y)$	8.71	8.31		0.0008
$7\,^1B_{1g}$ $(H\text{-}1 \rightarrow 3p_y)$	8.77	8.35		⋯
$6\,^1B_{2u}$ $(H \rightarrow 3p_x)$	9.07	8.42		0.0136
$6\,^1A_u$ $(H \rightarrow 3p_z)$	8.88	8.75		⋯
$4\,^1B_{2g}$ $(H\text{-}1 \rightarrow 3p_z)$	8.69	8.76		⋯
$8\,^1B_{1g}$ $(H \rightarrow 3d_{x^2-y^2})$	9.27	8.93		⋯
$5\,^1B_{3u}$ $(H\text{-}1 \rightarrow 3d_{x^2-y^2})$	9.02	9.12		0.0007
$9\,^1A_g$ $(H \rightarrow 3d_{xy})$	9.64	9.16		⋯
$6\,^1B_{1u}$ $(H\text{-}1 \rightarrow 3d_{xz})$	9.60	9.24		0.0006
$7\,^1B_{3g}$ $(H \rightarrow 3d_{xz})$	9.73	9.26		⋯
$7\,^1B_{2u}$ $(H\text{-}1 \rightarrow 3d_{xy})$	9.38	9.33		0.0023
$5\,^1B_{2g}$ $(H \rightarrow 3d_{yz})$	9.38	9.35		⋯
$7\,^1A_u$ $(H\text{-}1 \rightarrow 3d_{yz})$	9.14	9.44		⋯
$9\,^1B_{1g}$ $(H \rightarrow 3d_{z^2})$	9.64	9.53		⋯
$6\,^1B_{3u}$ $(H\text{-}1 \rightarrow 3d_{z^2})$	9.36	9.54		0.0089

TABLE III. (*Continued.*)

State	Excitation energies (eV) CASSCF	CASPT2	Exp.	Osc. Str.[a]
Triplet states				
$1\,^3B_{1g}$ (T_1, $n\pi^*$)	3.53	2.17	2.28[g], 2.31[h]	
$1\,^3A_u$ (T_2, $n\pi^*$)	3.55	2.27	2.32[b,g], 2.35[h]	
$1\,^3B_{1u}$ (T_3, $\pi\pi^*$)	3.41	2.91		
$1\,^3B_{3g}$ (T_4, $\pi\pi^*$)	3.82	3.19		

[a]Experimental values within parentheses. Three consecutive dots (⋯) represent forbidden states.
[b]Vapor phase absorption spectrum (Ref. 8).
[c]Excitation spectrum in a supersonic jet (Ref. 47).
[d]Vapor phase absorption spectrum (Ref. 9).
[e]Vacuum ultraviolet absorption spectrum (Ref. 46).
[f]Estimated value (Ref. 46).
[g]Vapor phase emission spectrum (Ref. 71).
[h]Pure crystal absorption spectrum (Ref. 66).

instance, MRSDCI calculations yielded a separation between the two lowest $n\pi^*$ states of 0.03 eV. The MRSDCI excitation energies exhibited, however, deviations of 0.5–0.6 eV.[11] Valence bond calculations underestimated the excitation energies with smaller deviations (0.3–0.4 eV) and led to splittings of about 100 cm^{-1}.[12,13]

b. The $1\,^1B_{3g}$ *and* $1\,^1B_{1u}$ *states.* In the near ultraviolet region of the spectrum, two features have been experimentally observed: a shoulder at about 4.1 eV, and a strong absorption around 5.1 eV. On the basis of simple molecular orbitals calculations and of the effect of chemical substitution on the position of these bands, Orgel[57] attributed these absorptions to the following $\pi\pi^*$ transitions: the weaker absorption to a $^1A_g \rightarrow {}^1B_{3g}$ excitation (forbidden) and the most intense one to a $^1A_g \rightarrow {}^1B_{1u}$ transition (allowed). Further studies on the direction of the transition moment by means of polarized light corroborated the assignment of the strongest band.[48,52,53]

These two states ($1\,^1B_{3g}$ and $1\,^1B_{1u}$) have been obtained in the present study as V_3 and V_6. The corresponding CASSCF wave functions possess a dominant singly excited $\pi \rightarrow \pi^*$ configuration: $1b_{1g} \rightarrow 2b_{2g}$ ($1\,^1B_{3g}$) and $2b_{3u} \rightarrow 2b_{2g}$ ($1\,^1B_{1u}$), which can be related to the $H \rightarrow L$ and $H\text{-}1 \rightarrow L$ one-electron promotions (see Fig. 1) , respectively. A second configuration exhibits a significant weight in the CASSCF wave functions of the two states. An electron is promoted from the same orbitals (H and H-1) to the second active orbital of the LUMO symmetry ($3b_{2g}$). The states have singly excited character, with a total weight of singly excited configurations larger than 60%. The computed vertical excitation energies for the $1\,^1A_g \rightarrow 1\,^1B_{3g}$ and $1\,^1A_g \rightarrow 1\,^1B_{1u}$ transitions are 4.19 and 5.15 eV, respectively, in agreement with the experimental data.[9]

Although the transition to the V_3 state is optically forbidden, a low intensity band corresponding to this transition has been observed.[46] Vibronic coupling between the V_3 and V_6 states has been suggested as the source of this nonvanishing feature.[9] The calculated oscillator strength for the transition to the V_6 state is found to be large. Indeed, the value is similar to the result obtained for the transition to the V_{14} state, which is related to the most intense feature of the observed spectrum (see below). There is an apparent discrepancy between the relative theoretical and experimental oscillator strength (cf. Table III). One has to bear in mind, however, that no vibronic coupling between V_3 and V_6 is included in the present theoretical description. Therefore, it is not surprising that an oscillator strength larger than expected is actually computed for the V_6 transition.

These $\pi\pi^*$ excited states have been previously calculated with SCF and CI methods.[10,11] The SCF procedure overestimated the excitation energies.[10,11] Addition of electron correlation by means of one-reference configuration interaction approaches did not lead to a significant improvement. For instance, at the SDCI/DZ level, the $^1B_{3g}$ state was placed at 5.30 eV, more than 1.2 eV higher than the observed value.[11] This error was even larger than the deviation obtained at the SCF level using the same basis set (0.96 eV). Likewise, the excitation energy computed for the $^1B_{1u}$ state at the SDCI/DZ level, 6.84 eV, is too high by 1.72 eV. Deviations are also seen for multireference SDCI results (0.42 and 0.99 eV).[11]

c. The $3\,^1B_{1u}$ *state.* The CASPT2 calculations predict the occurrence of an additional strong valence absorption band at 7.08 eV. It corresponds to the $1\,^1A_g \rightarrow 3\,^1B_{1u}$ transition with a large oscillator strength. The most important contribution to the wave function (see Table IV) is the $\pi - \pi^*$ one-electron promotion $1b_{1g} \rightarrow 1a_u$, which corresponds to an excitation from the HOMO to the second unoccupied π^* orbital. No previous *ab initio* calculation has been reported for this valence state.

Spectral information in this region is obtained from the ultraviolet absorption data reported by Brint *et al.*[46] Several intense peaks detected in the range 7–8 eV have been attributed to a valence transition at 7.0–7.1 eV and two Rydberg transitions at about 7.4 and 7.8 eV.[46] The valence feature was assigned to an allowed $\pi\pi^* {}^1A_g \rightarrow {}^1B_{1u}$ absorption originated by the one-electron excitation involving the $1b_{1g}$ and $1a_u$ orbitals. The assignment was supported by the results of two different semiempirical CNDO/S calculations,[58,59] which predicted the occurrence of an intense band in the energy range 7.3–7.6 eV. The results of these studies agree in the symmetry and nature of the excited

TABLE IV. CASSCF wave functions for *p*-benzoquinone: Number (weights) of singly (S), doubly (D), triply (T), and quadruply (Q) excited configurations[a] with coefficients larger than 0.05, principal configurations and weights.

State	No. conf. (weight) S	D	T	Q	Principal configurations	%
$1\,^1A_g$	3(12%)	16(11%)			$(1b_{3u})^2(1b_{2g})^2(5b_{2u})^2(4b_{3g})^2(2b_{3u})^2(1b_{1g})^2$	73
					$(1b_{2g})\rightarrow(3b_{2g})$	9
$1\,^1B_{1g}$	2(70%)	11(20%)	6(3%)	1(<1%)	$(4b_{3g})\rightarrow(2b_{2g})$	61
					$(5b_{2u})(2b_{3u})\rightarrow(2b_{2g})^2$	13
					$(5b_{2u})\rightarrow(3b_{3u})$	9
$1\,^1A_u$	2(70%)	11(18%)	6(3%)	1(<1%)	$(5b_{2u})\rightarrow(2b_{2g})$	61
					$(4b_{3g})(2b_{3u})\rightarrow(2b_{2g})^2$	13
					$(4b_{3g})\rightarrow(3b_{3u})$	9
$1\,^1B_{3g}$	6(65%)	15(26%)	2(1%)		$(1b_{1g})\rightarrow(2b_{2g})$	35
					$(1b_{1g})\rightarrow(3b_{2g})$	27
					$(1b_{2g})(1b_{1g})\rightarrow(2b_{2g})(3b_{2g})$	8
$2\,^1A_g$		8(82%)	12(11%)	2(1%)	$(4b_{3g})^2\rightarrow(2b_{2g})(3b_{2g})$	21
					$(5b_{2u})^2\rightarrow(2b_{2g})(3b_{2g})$	20
					$(4b_{3g})^2\rightarrow(2b_{2g})^2$	11
					$(5b_{2u})^2\rightarrow(2b_{2g})^2$	11
					$(4b_{3g})^2\rightarrow(3b_{2g})^2$	8
					$(5b_{2u})^2\rightarrow(3b_{2g})^2$	8
$1\,^1B_{2g}$	1(27%)	16(56%)	9(6%)	2(1%)	$(5b_{2u})\rightarrow(1a_u)$	27
					$(4b_{3g})(1b_{1g})\rightarrow(2b_{2g})(3b_{2g})$	12
					$(4b_{3g})(1b_{1g})\rightarrow(2b_{2g})^2$	11
					$(4b_{3g})(2b_{3u})\rightarrow(1a_u)(3b_{2g})$	8
					$(5b_{2u})(1b_{1g})\rightarrow(2b_{2g})(3b_{3u})$	8
					$(4b_{3g})(2b_{3u})\rightarrow(2b_{2g})(1a_u)$	7
$1\,^1B_{1u}$	5(77%)	16(14%)	5(2%)		$(2b_{3u})\rightarrow(2b_{2g})$	44
					$(2b_{3u})\rightarrow(3b_{2g})$	26
$1\,^1B_{3u}$	2(32%)	17(52%)	11(6%)	1(<1%)	$(4b_{3g})\rightarrow(1a_u)$	31
					$(5b_{2u})(1b_{1g})\rightarrow(2b_{2g})(3b_{2g})$	10
					$(5b_{2u})(1b_{1g})\rightarrow(2b_{2g})^2$	10
					$(5b_{2u})(2b_{3u})\rightarrow(1a_u)(3b_{2g})$	5
$2\,^1B_{2g}$	1(34%)	16(50%)	15(6%)		$(5b_{2u})\rightarrow(1a_u)$	34
					$(4b_{3g})(1b_{1g})\rightarrow(2b_{2g})^2$	18
					$(4b_{3g})(1b_{1g})\rightarrow(2b_{2g})(3b_{2g})$	12
$2\,^1B_{1g}$	3(30%)	16(57%)	8(4%)	2(1%)	$(5b_{2u})\rightarrow(3b_{3u})$	27
					$(5b_{2u})(2b_{3u})\rightarrow(2b_{2g})^2$	24
					$(1b_{2g})(4b_{3g})\rightarrow(2b_{2g})^2$	15
					$(4b_{3g})(2b_{3u})\rightarrow(2b_{2g})(3b_{3u})$	9
$2\,^1A_u$	3(28%)	13(58%)	11(4%)	2(<1%)	$(4b_{3g})\rightarrow(3b_{3u})$	26
					$(4b_{3g})(2b_{3u})\rightarrow(2b_{2g})^2$	25
					$(1b_{2g})(5b_{2u})\rightarrow(2b_{2g})^2$	16
					$(5b_{2u})(2b_{3u})\rightarrow(2b_{2g})(3b_{3u})$	9
$3\,^1A_g$	3(20%)	26(65%)	10(5%)	1(<1%)	$(2b_{3u})^2\rightarrow(2b_{2g})(3b_{2g})$	15
					$(2b_{3u})^2\rightarrow(2b_{2g})^2$	13
					$(1b_{2g})\rightarrow(2b_{2g})$	12
					$(1b_{1g})^2\rightarrow(2b_{2g})^2$	6
					$(2b_{3u})\rightarrow(3b_{3u})$	6
$2\,^1B_{3g}$	5(63%)	13(26%)	8(4%)	1(<1%)	$(2b_{3u})\rightarrow(1a_u)$	52
					$(1b_{2g})(2b_{3u})\rightarrow(1a_u)(3b_{2g})$	10
					$(1b_{1g})\rightarrow(2b_{2g})$	5
$1\,^1B_{2u}$	3(22%)	23(62%)	11(6%)	2(1%)	$(1b_{1g})\rightarrow(3b_{3u})$	14
					$(2b_{3u})(1b_{1g})\rightarrow(2b_{2g})(3b_{2g})$	10
					$(2b_{3u})(1b_{1g})\rightarrow(2b_{2g})^2$	8
					$(1b_{2g})\rightarrow(1a_u)$	7
					$(2b_{3u})^2\rightarrow(1a_u)(3b_{2g})$	7
					$(1b_{3u})(1b_{1g})\rightarrow(2b_{2g})(3b_{2g})$	6
					$(1b_{2g})(1b_{1g})\rightarrow(2b_{2g})(3b_{3u})$	5
$3\,^1B_{1u}$	4(71%)	8(15%)	11(8%)		$(1b_{1g})\rightarrow(1a_u)$	69
					$(1b_{2g})(1b_{1g})\rightarrow(1a_u)(3b_{2g})$	7
$4\,^1B_{1u}$	6(35%)	20(52%)	8(4%)	2(1%)	$(1b_{3u})\rightarrow(2b_{2g})$	22
					$(2b_{3u})(1b_{2g})\rightarrow(2b_{2g})(3b_{2g})$	10
					$(1b_{3u})\rightarrow(3b_{2g})$	8
					$(2b_{3u})(1b_{2g})\rightarrow(2b_{2g})^2$	8
					$(2b_{3u})^2\rightarrow(2b_{2g})(3b_{3u})$	6
$4\,^1B_{1g}$	3(11%)	17(68%)	11(8%)	2(1%)	$(5b_{2u})(1b_{1g})\rightarrow(2b_{2g})(1a_u)$	20
					$(1b_{3u})(5b_{2u})\rightarrow(2b_{2g})^2$	19

TABLE IV. (*Continued.*)

State	No. conf. (weight) S	D	T	Q	Principal configurations	%
					$(1b_{2g})(4b_{3g})\rightarrow(2b_{2g})^2$	8
					$(4b_{3g})\rightarrow(4b_{2g})$	6
$4\ ^1A_u$	3(16%)	16(64%)	6(6%)	3(1%)	$(1b_{3u})(4b_{3g})\rightarrow(2b_{2g})^2$	17
					$(4b_{3g})(1b_{1g})\rightarrow(2b_{2g})(1a_u)$	17
					$(5b_{2u})\rightarrow(4b_{2g})$	11
					$(1b_{2g})(5b_{2u})\rightarrow(2b_{2g})^2$	8
					$(5b_{2u})(1b_{1g})\rightarrow(1a_u)(3b_{3u})$	5
$5\ ^1A_g$	3(12%)	20(68%)	14(10%)		$(1b_{1g})^2\rightarrow(2b_{2g})^2$	15
					$(2b_{3u})(1b_{1g})\rightarrow(2b_{2g})(1a_u)$	11
					$(1b_{1g})^2\rightarrow(1a_u)^2$	8
					$(1b_{3u})(2b_{3u})\rightarrow(2b_{2g})^2$	8
					$(1b_{2g})\rightarrow(2b_{2g})$	7
					$(1b_{3u})(2b_{3u})\rightarrow(2b_{2g})(3b_{2g})$	5
$6\ ^1A_g$		2(75%)	16(15%)	7(3%)	$(5b_{2u})(4b_{3g})\rightarrow(3b_{3u})(3b_{2g})$	43
					$(5b_{2u})(4b_{3g})\rightarrow(3b_{3u})(2b_{2g})$	32

[a]With respect to the ground-state principal configuration.

state implied (here $3\ ^1B_{1u}$), although they differ substantially in the relative intensity of the band. Merienne-Lafore and Trommsdorff[58] calculated an oscillator strength smaller than that computed for the intense band at 5.1 eV, but a reverse trend was reported by Bigelow.[59]

The CASPT2 results give full support to the assignment proposed by Brint *et al.*[46] The $3\ ^1B_{1u}$ state (V_{14}) is computed to be 7.08 eV above the ground state, in excellent agreement with the experimental data. The additional valence transitions predicted in this region, V_{13} ($1\ ^1B_{2u}$) and V_{15} ($4\ ^1B_{1u}$), appear at 6.89 and 7.24 eV, respectively, but both have small oscillator strengths. Consequently, contribution of the V_{13} and V_{15} states to the observed band are predicted to be negligible. The large difference between the excitation energies for the V_{14} state obtained at the CASSCF (10.45 eV) and CASPT2 (7.08 eV) levels indicates the importance of the dynamic correlation effects for the correct description of this excited state. The assignment proposed is also supported by the following reasoning. The main orbitals describing the $3\ ^1B_{1u}$ state, $1b_{1g}$ and $1a_u$, have no contribution from the carbonyl groups. They are primarily the out-of-phase combination of the bonding and antibonding π orbitals of the C=C bonds (cf. Fig. 1). Topologically, the orbitals are similar to the corresponding MOs in 1,4-cyclohexadiene. A combined experimental and theoretical investigation of the electronic spectra of this molecule has been recently reported.[60] One of the excited states studied in that work, V_2 ($1\ ^1B_{3u}$), has a principal one-electron configuration which is analogous to that found for the V_{14} state of *p*-benzoquinone. The corresponding excitation energies are similar for the two systems. The CASSCF/CASPT2 results are 10.47/7.16 eV for 1,4-cyclohexadiene and 10.45/7.08 eV for *p*-benzoquinone. The CASPT2 findings are in agreement with the experimental data.[46,61]

d. Additional valence singlet excited states. In addition to the five excited states presented so far (V_1, V_2, V_3, V_6, and V_{14}), fourteen singlet valence states have been calculated and the results are also included in Tables III and IV. They lie within the energy range 4.4–7.9 eV above the ground state. Most of the states are related to optically forbidden transitions and those allowed (V_7, V_{13}, and V_{15}) exhibit small oscillator strengths. The corresponding wave functions have important differences with respect to the five states already analyzed. The largest weight for the additional 14 states comes from the set of doubly excited configurations. The only exception is V_{12} (the $2\ ^1B_{3g}$ state), located at 6.34 eV, for which the weight of the singly excited configurations is 63%. This state is mainly described by the $2b_{3u} \rightarrow 1a_u$ one-electron promotion, i.e., the excitation from *H*-1 to the second π^* orbital. Most of the excited states have a pronounced doubly excited multiconfigurational character with a one-electron promotion as the principal configuration. In particular, it holds true for the V_5, V_7, V_8, V_9, V_{10}, V_{13}, and V_{15} states.

The *ab initio* excitation energies reported by Ha[11] differ from the present CASPT2 findings. For instance, at the MRSDCI level, the excitation energies for the states labeled here as V_7, V_{12}, and V_{13} were computed to be 7.07, 7.75, and 8.47 eV, respectively. The corresponding values obtained at the CASPT2 level are 5.15, 6.34, and 6.89 eV. The CI transition energies are more than 1 eV higher than the CASPT2 results, but closer to the CASSCF values. The available semiempirical results, for instance at the CNDO/S level,[58,59] are closer to the CASPT2 values.

Regarding the valence excited states which have a principal doubly excited configuration, the wave functions also exhibit a multiconfigurational character. The $2\ ^1A_g$ state (V_4) appears at 4.41 eV, below the first intense $\pi\pi^*$ band. The $3\ ^1A_g$ state (V_{11}), at 5.90 eV, is located between the two strong $\pi\pi^*$ absorptions. The V_{16}–V_{19} states are placed within the energy range 7.3–7.9 eV. As far as we know, theoretical results for these excited states have not been previously reported.

2. Rydberg excited singlet states

Rydberg states converging to the four ionization limits are expected to overlap in energy, even for early series mem-

bers. In the present work, the states described by excitations out of H, H-1, n_-, and n_+ to the $3s$ and to the different components of the $3p$ and $3d$ Rydberg orbitals are examined.

a. *$n\rightarrow$ 3s and $n\rightarrow$ 3p states.* The lowest-energy Rydberg singlet states occur in the energy interval 6.5–7.5 eV. These states represent excitations from the n orbitals to the $3s$ and $3p$ functions. The $3\,^1B_{3g}$ state, described by the one-electron promotion $n_-\rightarrow 3s$, is obtained as the lowest Rydberg singlet state. The calculated excitation energy is 6.53 eV and the transition is dipole forbidden. Three additional Rydberg states have been calculated close to the valence state responsible for the most intense band of the spectrum (V_{14}). They are the $2\,^1B_{1u}$ ($n_-\rightarrow 3p_y$), $4\,^1A_g$ ($n_+\rightarrow 3p_y$), and $2\,^1B_{2u}$ ($n_+\rightarrow 3s$) states, with transition energies 6.86, 7.08, and 7.10 eV, respectively. The second state is forbidden. The first and the third states exhibit small computed oscillator strengths. Between 7.2 and 7.4 eV, three forbidden Rydberg transitions are obtained. The corresponding excited states involved are $4\,^1B_{3g}$ ($n_+\rightarrow 3p_z$), $3\,^1B_{1g}$ ($n_+\rightarrow 3p_x$), and $3\,^1A_u$ ($n_-\rightarrow 3p_x$). In addition, the $3\,^1B_{2u}$ ($n_-\rightarrow 3p_z$) state appears at 7.44 eV and is predicted to have a small oscillator strength.

The vacuum ultraviolet absorption spectrum analyzed by Brint *et al.*,[46] shows in this region a sharp peak at about 7.4 eV, with an estimated oscillator strength of 0.03. They attributed this absorption to the lowest-energy member of a p-type series and suggested that it probably has p_z character. In view of the results obtained here at the CASPT2 level, the only candidate for this absorption is the $3\,^1B_{2u}$ ($n_-\rightarrow 3p_z$) state, computed to be at 7.44 eV. Thus, the results support the assignment proposed by Brint *et al.*[46]

The dipole-allowed transition to the $2\,^1B_{1u}$ ($n_-\rightarrow 3p_y$) state, which appears at 6.86 eV, has not been previously assigned. Transitions to the p_y orbitals were proposed by Brint *et al.* as responsible for a weak feature at about 7.7 eV. In the light of the CASPT2 results, however, this assignment can be ruled out. Probably, it is masked by the intense valence band located at 7.1 eV.

No evidence of s-type absorptions has been found in the measured spectrum.[46] The two possible candidates for the lowest $3s$ feature can be related to the states involving the n_- and n_+ orbitals, i.e., the $3\,^1B_{3g}$ and $2\,^1B_{2u}$ states, respectively. Transition to the former is forbidden. Actually, it is not observed. Nevertheless, when reductions of the molecular symmetry are carried out by replacing hydrogen atoms with methyl groups, the observed spectra show an absorption feature between 6.5 and 7 eV.[62] The peak has been assigned to a $3s$ Rydberg transition.[62] The excitation energy computed for the $3\,^1B_{3g}$ ($n_-\rightarrow 3s$) state, 6.53 eV, is within that energy range. In contrast, the oscillator strength value for the optically allowed $2\,^1B_{2u}$ ($n_+\rightarrow 3s$) state, placed at 7.10 eV, is computed to be small.

b. $n\rightarrow$3d and $\pi\rightarrow$3s states. The first Rydberg state above 7.5 eV is the $5\,^1B_{3g}$ ($n_-\rightarrow 3d_{x^2-y^2}$). This is the first member of the $n\rightarrow 3d$ series, which is found between 7.5 and 8.2 eV. Ten $n\rightarrow 3d$ states have been calculated, but only one of the allowed transitions, that involving the $5\,^1B_{1u}$ ($n_+\rightarrow 3d_{yz}$) state, has a non-negligible oscillator strength. It should be noted, however, that the first members of the series from the H and H-1 π orbitals also appear in the same energy range. The $5\,^1B_{1g}$ ($H\rightarrow 3s$) and $2\,^1B_{3u}$ (H-1 $\rightarrow 3s$) states have excitation energies of 7.70 and 8.01 eV, respectively. The former is forbidden, while the latter is allowed.

From an experimental point of view, a band has been detected in this region at about 7.8 eV with an estimated oscillator strength of 0.03.[46] It has been assigned to $n\rightarrow 3d$ transitions.[46] The band appears to be a doublet. The two d states have been suggested to be of different symmetry. According to the excitation energies obtained at the CASPT2 level, three allowed transitions could be responsible for this feature: $1\,^1A_g\rightarrow 5\,^1B_{1u}$ ($n_+\rightarrow 3d_{yz}$), $1\,^1A_g\rightarrow 4\,^1B_{2u}$ ($n_+\rightarrow 3d_{x^2-y^2}$), and $1\,^1A_g\rightarrow 2\,^1B_{3u}$ (H-1$\rightarrow 3s$). The corresponding computed vertical excitation energies are 7.79, 7.87, and 8.01 eV, respectively. The second electronic transition exhibits a small value of oscillator strength (0.0002), while the results for the other two transitions are more than a hundred times larger (0.0290 and 0.0246). Consequently, the electronic transition with the smallest oscillator strength can be excluded as candidate for the assignment of this band. Therefore, in the light of the CASPT2 results, one can conclude that the absorption band is due to two different electronic transitions, involving states of different symmetry and nature, $5\,^1B_{1u}$ and $2\,^1B_{3u}$. Whereas one does belong to the d-type series, the other feature does not; it is a $3s$-type transition.

The theoretical interpretation does not support the conclusion proposed by Brint *et al.*[46] concerning the character of the observed Rydberg bands. On the basis of a rough estimation of the total Rydberg oscillator strength and its comparison with the corresponding value measured for benzene, formaldehyde, and acetone, they concluded that the observed Rydberg series of p-benzoquinone are ketonic, involving the n orbitals localized in the carbonyl groups, rather than benzenoid, involving the π orbitals. Therefore, they assumed that the Rydberg series originate from the n_- molecular orbitals (assignments based on the n_+ orbital would apply equally well) and accordingly gave an interpretation of all the observed bands. The possibility of an assignment involving the π orbitals was thus completely discarded.[46] The CASPT2 results suggest, however, that this possibility should not be excluded. The interpretation of the spectrum seems to be more adequate when both type of Rydberg transitions are taken into account.

c. $\pi\rightarrow$3p and $\pi\rightarrow$3d states. The Rydberg states described by excitations from H and H-1 to the $3p$ orbitals are computed to lie 8.15–8.80 eV above the ground state. As can be seen in Table III, two transitions are allowed. Only the transition involving the $6\,^1B_{2u}$ ($H\rightarrow 3p_x$) state exhibits a significant oscillator strength. The corresponding excitation energy is 8.42 eV. In the energy interval 8.9–9.6 eV, the $\pi\rightarrow 3d$ states appear, which are predicted to have a low oscillator strength. It should be noted, however, that a full theoretical assignment of the spectrum in this region cannot at present be achieved. Further members of the different series, which are not considered in the current investigation, are expected to lie close to the computed states.

3. Triplet excited states

In the study of the absorption spectrum of *p*-benzoquinone at low temperature in the crystalline state, Sidman proposed that a very weak absorption system detected slightly below the lowest-energy singlet–singlet bands could be related to a singlet–triplet $n\rightarrow\pi^*$ transition.[52] Subsequently, these bands as well as the nature of the lowest triplet valence states have been exhaustively examined by means of a large variety of techniques in different environments. A detailed description of all these experimental studies can be found elsewhere (see Refs. 6, 9, and references cited therein). The information provided by these investigations led to important conclusions. The triplet character of the excited state involved in such low-energy band was proven.[63,64] The absorption was assigned to a $^1A_g\rightarrow{}^3A_u$ ($n\pi^*$) transition; spin-orbit interaction was suggested as the responsible mechanism for the observed intensity.[8,65] Nevertheless, a new controversy arose. The absorption spectrum of *p*-benzoquinone in the crystal showed an additional even weaker band located 0.04 eV below the $^1A_g\rightarrow{}^3A_u$ transition.[66] The new feature was attributed to a different electronic transition and two possible assignments were proposed,[9,66] either a $\pi\pi^*$ $^1A_g\rightarrow{}^3B_{1u}$ or an $n\pi^*$ $^1A_g\rightarrow{}^3B_{1g}$ transition. Trommsdorff[9] proved that only the second assignment was compatible with the experimental data. He concluded that the lowest triplet is the $n\pi^*$ $^3B_{1g}$ state, with the $n\pi^*$ ^3A_u state located slightly above, and that the $\pi\pi^*$ $^3B_{1u}$ state lies at still higher energy above the $n\pi^*$ $^1B_{1g}$ state. The assignment of the lowest-energy triplet state was further confirmed by other spectroscopic techniques both for pure and mixed crystals.[6,67–70] In the vapor phase, the transition to the $^3B_{1g}$ state has not been identified in the absorption spectrum.[6] A weak phosphorescence band, placed 0.04 eV below that corresponding to the $^3A_u\rightarrow{}^1A_g$ emission, was observed by Koyanagi *et al.*[71] It was attributed to a $^3B_{1g}\rightarrow{}^1A_g$ transition. This band has not been unambiguously observed in more recent studies.[6]

Theoretical determination of the lowest triplet state has been controversial and still remains unresolved. It has been predicted a $\pi\pi^*$ $^3B_{1u}$[45,58] or an $n\pi^*$ $^3B_{1g}$ state[7] by semiempirical methods, depending on the approach. At the SCF, SCI, and MRSDCI levels, the lowest triplet state is calculated to be the $\pi\pi^*$ $^3B_{1u}$ state[10,11], which is in contradiction to the experimental evidence.[6,9,67–71] In order to get further insight into the nature of the lowest triplet state, the two $n\pi^*$ states ($^3B_{1g}$ and ^3A_u) and the two $\pi\pi^*$ states ($^3B_{1u}$ and $^3B_{3g}$) have been calculated with the CASSCF/CASPT2 procedure. The CASSCF calculations were carried out with valence active spaces, (8/03010301) for the $\pi\pi^*$ states and (12/03110311) for the $n\pi^*$ states, employing the C,O $[4s3p1d]$/H$[2s1p]$ basis set.

The triplet states considered are described by the same main singly excited configuration as the corresponding singlet state. At the CASSCF level, the lowest triplet state is predicted to be the $\pi\pi^*$ $^3B_{1u}$ state (cf. Table III), as in previous *ab initio* studies. The ordering of the states changes when dynamic correlation effects are included by the second-order treatment. The CASPT2 procedure places the $n\pi^*{}^3B_{1g}$ as the lowest triplet state. The computed transition energies for the two $n\pi^*$ states, 2.17 eV ($^1A_g\rightarrow{}^3B_{1g}$) and 2.27 eV ($^1A_g\rightarrow{}^3A_u$) correlate well with the available experimental data (cf. Table III). The finding that the $^3B_{1g}$ state is related to the lowest-energy electronic transition is consistent with the experimental evidence obtained in the crystal and from vapor phase emission spectra.[6,9,67–71] Moreover, since the present computation was performed *in vacuo*, the $n\pi^*$ $^3B_{1g}$ state can also be predicted as the lowest in the vapor phase. Further experimental investigations would be helpful in order to confirm our prediction.

Transitions to the $\pi\pi^*$ $^3B_{1u}$ and $^3B_{3g}$ states are computed to be at 2.91 and 3.19 eV, respectively. Therefore, they are found at higher energies than the $n\pi^*$ states. The energy difference between the triplet states of $n\pi^*$ and $\pi\pi^*$ type (>0.6 eV) is large enough to determine unambiguously the $n\pi^*$ character of the lowest triplet state *in vacuo*. It is also worth noting that the CASPT2 results locate the $\pi\pi^*$ triplet states above the lowest $n\pi^*$ singlet states, in agreement with the interpretation by Trommsdorff.[9] Regarding the computed singlet–triplet splittings, they are found to be larger for the $\pi\pi^*$ states than for the $n\pi^*$ states (cf. Table III). In a simple MO model, the splitting can be related to the magnitude of the exchange integral involving the two MOs of the excitation. The fact that this value is larger for $\pi\rightarrow\pi^*$ than for $n\rightarrow\pi^*$ excitations rationalizes the computed singlet–triplet splittings.

IV. CONCLUSIONS

We have presented results from an *ab initio* study of the electronic spectrum of *p*-benzoquinone. The study has been performed with multiconfigurational second-order perturbation theory using the CASPT2 method. The results enable the understanding of the main features of the spectrum. The computed valence singlet–singlet transition energies agree with the available experimental data. Certain assignments proposed earlier have been confirmed. The absorption in the visible region is due to $n\pi^*$ $^1A_g\rightarrow{}^1B_{1g}$ and $^1A_g\rightarrow{}^1A_u$ electronic transitions and the bands in the near ultraviolet correspond to $\pi\pi^*$ $^1A_g\rightarrow{}^1B_{3g}$ and $^1A_g\rightarrow{}^1B_{1u}$ excitations. The most intense band observed around 7.1 eV is attributed to a $\pi\pi^*$ $^1A_g\rightarrow{}^1B_{1u}$ transition. The results obtained for the Rydberg singlet states make it possible to assign the bands detected at about 7.4 and 7.8 eV. The former corresponds to an $n\rightarrow 3p$ excitation, whereas two transitions of different character ($n\rightarrow 3d$ and $\pi\rightarrow 3s$) are involved in the latter. In addition, the $n\pi^*$ $^3B_{1g}$ state is predicted to be the lowest triplet state, in agreement with available experimental findings. The $\pi\pi^*$ $^3B_{1u}$ state has been computed to lie more than 0.7 eV above the lowest triplet state, $n\pi^*$ $^3B_{1g}$, and is located above the two lowest $n\pi^*$ singlet states.

ACKNOWLEDGMENTS

The research reported in this communication has been supported by the projects PB95-0428-C02 and PB97-1377 of Spanish DGES-MEC and by the European Commission through the TMR network FMRX-CT96-0079.

[1] L. Stryer, *Biochemistry* (W. H. Freeman & Co., New York, 1995).
[2] J. P. Klinman and D. Mu, Annu. Rev. Biochem. **63**, 299 (1994).
[3] J. W. Lown, Chem. Soc. Rev. **22**, 165 (1993).
[4] V. Khodorkovsky and J. Y. Becker, in *Organic Conductors*, edited by J.-P. Farges (Marcel Dekker, New York, 1994), p. 75.
[5] L. Light, Z. Phys. Chem., Stoechiom. Verwandtschaftsl. **122**, 414 (1926). During the first three decades of this century, earlier qualitative studies of the electronic spectrum of *p*-benzoquinone were also reported. Details can be found in this reference.
[6] T. Itoh, Chem. Rev. **95**, 2351 (1995).
[7] N. J. Bunce, J. E. Ridley, and M. C. Zerner, Theor. Chim. Acta **45**, 283 (1977).
[8] J. M. Hollas, Spectrochim. Acta **20**, 1563 (1964).
[9] H. P. Trommsdorff, J. Chem. Phys. **56**, 5358 (1972).
[10] M. H. Wood, Theor. Chim. Acta **36**, 345 (1975).
[11] T.-K. Ha, Mol. Phys. **49**, 1471 (1983).
[12] R. L. Martin, J. Chem. Phys. **74**, 1852 (1981).
[13] R. L. Martin and W. R. Wadt, J. Phys. Chem. **86**, 2382 (1982).
[14] J. R. Ball and C. Thomson, Theor. Chim. Acta **74**, 195 (1988).
[15] P. Mohandas and S. Umapathy, J. Phys. Chem. A **101**, 4449 (1997).
[16] L. A. Eriksson, F. Himo, P. E. M. Siegbahn, and G. T. Babcock, J. Phys. Chem. A **101**, 9496 (1997).
[17] K. Andersson, P.-Å Malmqvist, B. O. Roos, A. J. Sadlej, and K. Wolinski, J. Phys. Chem. **94**, 5483 (1990).
[18] K. Andersson, P.-Å Malmqvist, and B. O. Roos, J. Chem. Phys. **96**, 1218 (1992).
[19] K. Andersson and B. O. Roos, in *Advanced Series in Physical Chemistry; Modern Electron Structure Theory*, edited by R. Yarkony (World Scientific, Singapore, 1995), Vol. 2, part I, p. 55.
[20] B. O. Roos, M. P. Fülscher, P.-Å. Malmqvist, M. Merchán, and L. Serrano-Andrés, in *Quantum Mechanical Electronic Structure Calculations with Chemical Accuracy*, edited by S. R. Langhoff (Kluwer Academic, Dordrecht, The Netherlands, 1995), p. 357.
[21] B. O. Roos, K. Andersson, M. P. Fülscher, P.-Å. Malmqvist, L. Serrano-Andrés, K. Pierloot, and M. Merchán, in *Advances in Chemical Physics; New Methods in Computational Quantum Mechanics*, edited by I. Prigogine and S. A. Rice (John Wiley & Sons, New York, 1996), Vol. XCIII, p. 219.
[22] M. Merchán, L. Serrano-Andrés, M. P. Fülscher, and B. O. Roos, in *Recent Advances in Multireference Theory*, edited by K. Hirao (World Scientific, Amsterdam, 1998).
[23] B. O. Roos, in *Advances in Chemical Physics; Ab Initio Methods in Quantum Chemistry - II*, edited by K. P. Lawley (John Wiley & Sons, Chichester, England, 1987), Chap. 69, p. 399.
[24] K. Hagen and K. Hedberg, J. Chem. Phys. **59**, 158 (1973).
[25] P.-O. Widmark, P.-Å Malmqvist, and B. O. Roos, Theor. Chim. Acta **77**, 291 (1990).
[26] M. Merchán and B. O. Roos, Theor. Chim. Acta **92**, 227 (1995).
[27] M. Merchán, B. O. Roos, R. McDiarmid, and X. Xing, J. Chem. Phys. **104**, 1791 (1996).
[28] P.-Å Malmqvist, Int. J. Quantum Chem. **30**, 479 (1986).
[29] P. Å. Malmqvist and B. O. Roos, Chem. Phys. Lett. **155**, 189 (1989).
[30] MOLCAS, Version 4.0, K. Andersson, M. R. A. Blomberg, M. P. Fülscher, G. Karlström, R. Lindh, P.-Å. Malmqvist, P. Neogrády, J. Olsen, B. O. Roos, A. J. Sadlej, M. Schütz, L. Seijo, L. Serrano-Andrés, P. E. M. Siegbahn, and P.-O. Widmark, University of Lund, 1997.
[31] R. M. Stevens, E. Switkes, E. A. Laws, and W. N. Libscomb, J. Am. Chem. Soc. **93**, 2603 (1971).
[32] G. Dallinga and L. H. Toneman, J. Mol. Struct. **1**, 117 (1967).
[33] H. Oberhammer and S. H. Bauer, J. Am. Chem. Soc. **91**, 10 (1969).
[34] R. Nelson and L. Pierce, J. Mol. Spectrosc. **18**, 344 (1965).
[35] L. Serrano-Andrés, R. Lindh, B. O. Roos, and M. Merchán, J. Phys. Chem. **97**, 9360 (1993).
[36] V. Molina, M. Merchán, and B. O. Roos, J. Phys. Chem. A **101**, 3478 (1997).
[37] R. Liu, X. Zhou, and P. Pulay, J. Phys. Chem. **96**, 4255 (1992).
[38] S. E. Boesch and R. A. Wheeler, J. Phys. Chem. **99**, 8125 (1995).
[39] M. Nonella and P. Tavan, Chem. Phys. **199**, 19 (1995).
[40] C.-G. Zhan and S. Iwata, Chem. Phys. **230**, 45 (1998).
[41] Y. Yamakita and M. Tasumi, J. Phys. Chem. **99**, 8524 (1995).
[42] X. Zhao, H. Imahori, C.-G. Zhan, Y. Mizutani, Y. Sakata, and T. Kitagawa, Chem. Phys. Lett. **262**, 643 (1996).
[43] Y. H. Mariam and L. Chantranupong, J. Comput.-Aided Mol. Design **11**, 345 (1997).
[44] M. Braga and S. Larsson, Chem. Phys. **162**, 369 (1992), and references cited therein.
[45] L. Åsbrink, G. Bieri, C. Fridh, E. Lindholm, and D. P. Chong, Chem. Phys. **43**, 189 (1979).
[46] P. Brint, J.-P. Connerade, P. Tsekeris, A. Bolovinos, and A. Baig, J. Chem. Soc., Faraday Trans. 2 **82**, 367 (1986).
[47] G. Ter Horst and J. Kommandeur, Chem. Phys. **44**, 287 (1979).
[48] J. C. D. Brand and T. H. Goodwin, Trans. Faraday Soc. **53**, 295 (1957).
[49] T. Anno, A. Sado, and I. Matubara, J. Chem. Phys. **26**, 967 (1957).
[50] R. K. Asundi and R. S. Singh, Nature (London) **176**, 1223 (1955).
[51] T. Anno and A. Sado, J. Chem. Phys. **32**, 1602 (1960).
[52] J. W. Sidman, J. Am. Chem. Soc. **78**, 2363 (1956).
[53] J. W. Sidman, J. Chem. Phys. **27**, 820 (1957).
[54] H. P. Trommsdorff, Chem. Phys. Lett. **10**, 176 (1971).
[55] T. M. Dunn and A. H. Francis, J. Mol. Spectrosc. **50**, 14 (1974).
[56] J. Goodman and L. E. Brus, J. Chem. Phys. **69**, 1604 (1978).
[57] L. E. Orgel, Trans. Faraday Soc. **52**, 1172 (1956).
[58] M. F. Merienne-Lafore and H. P. Trommsdorff, J. Chem. Phys. **64**, 3791 (1976).
[59] R. W. Bigelow, J. Chem. Phys. **68**, 5086 (1978).
[60] M. Merchán, L. Serrano-Andrés, L. S. Slater, B. O. Roos, and R. McDiarmid, J. Phys. Chem. A (in press).
[61] R. McDiarmid and J. P. Doering, J. Chem. Phys. **75**, 2687 (1981).
[62] P. Brint, P. Tsekeris, A. Bolovinos, and C. Kosmidis, J. Chem. Soc., Faraday Trans. 2 **85**, 177 (1989).
[63] W. H. Eberhardt and H. Renner, J. Mol. Spectrosc. **6**, 483 (1961).
[64] H. P. Trommsdorff, Chem. Phys. Lett. **1**, 214 (1967).
[65] J. M. Hollas and L. Goodman, J. Chem. Phys. **43**, 760 (1965).
[66] M. Koyanagi, Y. Kogo, and Y. Kanda, J. Mol. Spectrosc. **34**, 450 (1970).
[67] H. Veenvliet and D. A. Wiersma, Chem. Phys. Lett. **22**, 87 (1973).
[68] A. I. Attia, B. H. Loo, and A. H. Francis, Chem. Phys. Lett. **22**, 537 (1973).
[69] S. J. Hunter, H. Parker, and A. H. Francis, J. Chem. Phys. **61**, 1390 (1974).
[70] H. Veenvliet and D. A. Wiersma, J. Chem. Phys. **60**, 704 (1974).
[71] M. Koyanagi, Y. Kogo, and Y. Kanda, Mol. Phys. **20**, 747 (1971).